# Aircraft Pipe Geometric Feature Modeling and Error Compensation Based on Assembly Constraints

**Yulong Lan**
Nanjing University of Aeronautics and Astronautics College of Economics and Management
**Songlin Chen**
AVIC ChengDu Aircraft Industrial (Group) Co., Ltd., Chendu 610092, China
**Wenxiang Gao** ( gao_scu@163.com )
AVIC Chengdu Aircraft Industrial (Group) Co., Ltd., Chengdu China. https://orcid.org/0000-0002-8233-1019
**Bangyi Li**
Nanjing University of Aeronautics and Astronautics College of Economics and Management
**Mutian Tang**
AVIC ChengDu Aircraft Industrial (Group) Co., Ltd., Chendu 610092, China

**Original Article**

**Keywords:** Assembly constraints, Feature modeling, Feature recognition, Error compensation

**Posted Date:** December 1st, 2020

**DOI:** https://doi.org/10.21203/rs.3.rs-116062/v1

## Title page

# Aircraft Pipe Geometric Feature Modeling and Error Compensation Based on Assembly Constraints

**Yu-Long LAN** received the B.S. and M.S. degrees from Sichuan University, Sichuan, China in 2000 and 2008 respectively. He is currently pursuing a PhD degree at Nanjing University of Aeronautics and Astronautics. Besides, he is an engineer in AVIC Chengdu Aircraft Industrial (Group) Co., Ltd., Chengdu China. His main research interests include the technology of aircraft assembly and Integrated Supply Chain (ISC).
E-mail: lanyl_2020@163.com

**Wen-Xiang GAO** received the B.S. and Ph.D. degree from Sichuan University, Sichuan, China in 2014 and 2019 respectively. He is currently an engineer in AVIC Chengdu Aircraft Industrial (Group) Co., Ltd., Chengdu, China. His main research interests include robot collision-free path planning, aircraft automatic assembling technology, application of industrial robot.
E-mail: gao_scu@163.com

Corresponding author：Wen-Xiang Gao　E-mail：gao_scu@163.com

ORIGINAL ARTICLE

# Aircraft Pipe Geometric Feature Modeling and Error Compensation Based on Assembly Constraints

**Yu-Long Lan[1, 2] • Song-Lin Chen[2] • Wen-Xiang Gao[2] • Bang-Yi Li[1] • Mu-Tian Tang[2]**

Received June xx, 201x; revised February xx, 201x; accepted March xx, 201x


**Abstract:** An error compensation method based on the assembly constraints of aircraft pipe is proposed for solving the problem of frequent failures caused by high assembly stress in the actual assembly process. Firstly, the pipe assembly process' geometric modeling is carried out using geometric modeling method, and a new modeling method based on axis vector is proposed. On this basis, the Rodrigues formula was used to establish a pipe space pose calculation model based on actual assembly conditions. Then, the assembly constraints are analyzed, and the key constraint features are identified based on the pipe assembly requirements. Subsequently, the pipe assembly scenarios under different constraint forms are analyzed, and the pipe error compensation methods under a single constraint and associated constraint are respectively proposed. Finally, a typical flaring pipe is selected for the test; the pipe assembly error compensation calculation and the pipe installation air tightness test are carried out respectively. The results show that the proposed method could effectively realize the theoretical space pose adjustment and the pipe parameter compensation, and the air tightness of the compensated pipe is better than that of the uncompensated one.
**Keywords:** Assembly constraints • Feature modeling • Feature recognition • Error compensation

## 1. Introduction

As the main part of aircraft, the metal pipe is widely used in the key structures of aircraft hydraulic, environmental control, fuel system, etc., and plays an important role in transmitting energy and power [1]. In the aircraft navigation, the subsystems inside the body start to work, and the pipe structure needs to bear high pressure and high-frequency vibration [2]. If there is a large pipe assembly error, it would lead to a great assembly stress in the pipe system, resulting in air leakage and oil leakage in the pipeline, and –causing malfunctions in subsystems of the aircraft, such as pressure loss, energy leakage and fire. Failures seriously affect the performance and safety of aircraft systems [3-4]. Therefore, the research of reducing the stress of pipe assembly and improving the quality of pipe installation has been concerned by scholars all over the world [5-7].

The pipe error composition includes the manufacturing error and the assembly error. The manufacturing error is caused by process of pipe manufacturing. In the study of pipe manufacturing error, Song et al. [8] established a prediction model between the manufacturing error and the pipe process parameters by using the multiple linear regression method. The prediction accuracy was controlled within 5%. The pipe assembly error consists of positioning error and structural assembly error. The positioning error is caused by guiding pipe assembly positioning, such as installation angle error and installation positioning error. The structural assembly

✉ Wen-Xiang Gao
gao_scu@163.com

[1] College of Economics and Management, Nanjing University of Aeronautics and Astronautics, Nanjing 210016, China

[2] AVIC ChengDu Aircraft Industrial (Group) Co., Ltd., Chendu 610092, China

error is the error of the reference structure of the installation pipe [9]. In the research of positioning error, Zhang et al. [10] studied the welding and assembly of the pipe based on the digital assembly angle. They analyzed the change rule of the angle between the flange and the pipe axis and proposed an active compensation method for the relative error of the pipe assembly via transferring the coordinate system of each section of the welded pipe into the reference coordinate system by using a special fixture. Zeng et al. [11] proposed the flexible positioning and clamping scheme of independent digital reconstruction fixture, using a matrix positioner to achieve the pipe positioning by controlling the end points of each straight line segment of the pipe. The above research has a good positioning effect for the welded pipe with flanges in the field of pipe manufacturing. However, in the non-flange pipe assembly application, as the manufacturing error cannot be eliminated completely, the theoretical coordinate points cannot be used to locate the catheter. Therefore, the existing method could not be effectively applied to the non-flange pipe assembly process.

A large error occurs in the overall structure assembly due to various factors, such as part manufacturing, assembly process, part stiffness and thermal restricting the pipe assembly accuracy [12]. Scholars civil and aboard have further study about structural assembly error. In terms of structural assembly error, Han et al. [13] established the pre-assembly error equation of large components by using the total differential method, and calculated the pre-assembly error of the aircraft structure under the analytical method. Cheng et al. [14] established a deformation-oriented aircraft digital assembly deviation model with theoretical analysis, mechanics and mathematical modeling, computational simulation and experimental verification, and realized the aircraft digital assembly deviation at a single station. The assembly deviation transmission model is given using the discrete system state equation, which reveals the transmission law of assembly deviation in aircraft digital assembly. Ding et al. [15] established the assembly error compensation model of 5-axis CNC machine tools using a homogeneous coordinate transformation matrix, which improved the compensation efficiency of assembly error of CNC machine tools. Ktithika et al. [16] realized the prediction of 99% gasket clearance of the whole aircraft by using machine learning and compressive sensing technology, and considered the distribution law of gasket clearance and assembly error in aircraft assembly. Qi et al. [17] analyzed the distribution law of aircraft structural error by using Monte Carlo method and finite element simulation, and established the mapping relationship between the actual error of wing structure and the theoretical model. Zhang et al. [18] used the laser tracker to measure and calculate the aircraft structural error after the structural assembly. Yu et al. [19] used the direct linearization method (DLM) to optimize the rocket engine pipe line assembly, gave the calculation formula of assembly limit deviation of spatial assembly dimension chain, and obtained the assembly sensitivity matrix through DLM.

At present, many studies focus on the improvement of manufacturing accuracy, positioning error control, structural error analysis and prediction of large components, while few studies have integrated the actual pipe into the structural assembly to improve the pipe actual assembly quality.

In this paper, an error compensation method based on pipe assembly characteristics is proposed to compensate and control the installation process. Firstly, the vector modeling of the pipe assembly process is established by using the geometric modeling method and Rodrigues formula [20]. On this basis, the assembly constraints are analyzed based on the assembly requirements, and the pipe assembly key features [21] are identified. Then, different pipe assembly scene is analyzed, and the pipe error compensation methods under single constraint and association constraint are proposed respectively. Finally, the error compensation calculation and air tightness test are carried out to verify the effectiveness of the proposed compensation method.

## 2. Assembly Feature Recognition

When two flaring pipes are installed, one end of two pipes are fixed on the aircraft structure separately, and the other end is connected by the threaded joint of the two pipes, to realize the sealing connection. Figure 1 shows the structure of two flared pipes assembly. The Pipe 1 could be expressed as an ordered set of points:

$$P_1 = \{A_1, A_2, \mathrm{L}\ , A_{n-1}, A_n\} \tag{1}$$

Similarly, the Pipe 2 could be expressed as:

$$P_2 = \{B_1, B_2, \mathrm{L}\ , B_{n-1}, B_n\} \tag{2}$$

where $O_1$ and $O_2$ respectively represent the installation positions of pipe 1 and pipe 2 on the aircraft structure. The $A_n$ and the $B_n$ of the two pipes are connected, and $A_n$ and $B_n$ respectively represent the point coordinates.

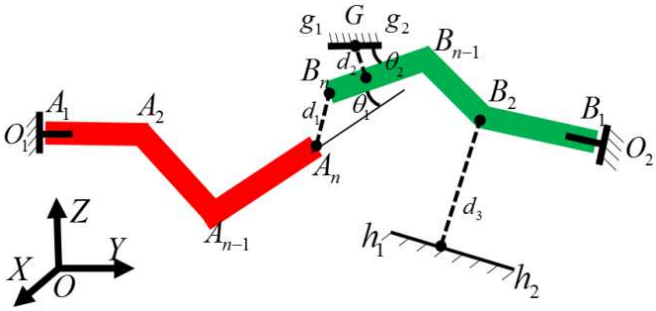


**Figure 1** 2D – Structural assembly sketch of pipeline.

In the actual assembly process, in order to ensure that the pipe is installed on the structure, it needs to meet the structural assembly constraints, including one basic condition and five assembly features. The basic conditions ensure that each pipe is fixed on the aircraft structure. The assembly features are divided into the angle and distance constraints at the butt of the two pipes, the angle and distance constraints on the middle part of the pipe by the clamp, and the clearance constraints on the pipe by the peripheral structure. The details are as follows:

(1) Basic conditions

The $A_1$ point of pipe 1 must coincide with the structure $O_1$, and the straight line $\overline{A_1A_2}$ is perpendicular to the end face of structure $O_1$. The pipe 2 meets the same requirements.

(2) Assembly features

1) Angle constraint: Pipe 1 and Pipe 2 meet the assembly angle constraint at the joint, that is, the angle $\theta_1$ between the line $\overline{A_{n-1}A_n}$ and the line $\overline{B_{n-1}B_n}$ must meet the theoretical constraint condition $\theta_1 \le [\theta_1]$, where $[\bullet]$ represents the theoretical value.

2) Distance constraint: the $A_n$ of pipe 1 and the $B_n$ of pipe 2 meet the distance constraint, $d_1 = |A_nB_n| \le [d_1]$.

3) Angle constraint: The angle $\theta_2$ between the clamp straight line $\overline{g_1g_2}$ and the pipe straight line $\overline{B_{n-1}B_n}$ must meet the theoretical constraint $\theta_2 \le [\theta_2]$.

4) Distance constraint: The distance from the center point $G$ of the clamp to the straight line $\overline{B_{n-1}B_n}$ of the pipe meets $d_2 \le [d_2]$.

5) Distance constraint: The distance $d_3$ between the pipe and the surrounding structure satisfies $|d_3 - h^*| \le [d_3]$.

The angle constraint $\theta_1$ and distance constraint $d_1$ are the main constraints to ensure the sealing performance of the butt joint. If these two constraints are not satisfied, it will lead to the pipe seal failure. This kind of problem has a high probability and needs to be considered first. Angle constraint $\theta_2$ and distance constraint $d_2$ reflect the position relationship between the fixed clamp and the pipe, which mainly affect the stress after the conduit assembly. When the stress is too large, it will cause problems, such as leakage and deformation, but the probability of such problems is low and the importance is less. The distance constraint $d_3$ is the distance between the surrounding structure and the pipe, and its theoretical value is defined as $h^*$. When the distance is too small, it will lead to the collision between the pipe and the surrounding structure in the flight process, resulting in the damage on the pipe. However, the probability of occurrence is lower, and the importance is the least.

## 3. Vector Modeling

The pipe vector modeling based on assembly features is carried out on the basis of feature recognition. Firstly, the pipe axis vector and its installation structure are extracted, and then the pipe vector model in actual assembly state is established.

### 3.1. Axis vector extraction

The flared pipe usually has redundant degrees of freedom (DOF) around the axis when connected with the fixed end of the aircraft structure. As shown in Figure 2, pipe 1 could be rotated around axis $\overline{A_1A_2}$. Based on the vector modeling of the pipe, the assembly process is controlled and optimized by using the rotation translation transformation of redundant DOF.

As shown in Figure 2, extract the pipe structural features, including pipe joint points, straight parts, turning points, and express them with vector sets:

$$\boldsymbol{a} = \{\boldsymbol{a}_1, \mathrm{L}\ , \boldsymbol{a}_n\} \tag{3}$$

$$\boldsymbol{b} = \{\boldsymbol{b}_1, \mathrm{L}\ , \boldsymbol{b}_n\} \tag{4}$$

The axis vector of the installation structure $O_1$ of the pipe 1 is denoted by $\boldsymbol{s}_1$, and the axis vector of the installation structure $O_2$ of the pipe 2 is denoted by $\boldsymbol{s}_2$.

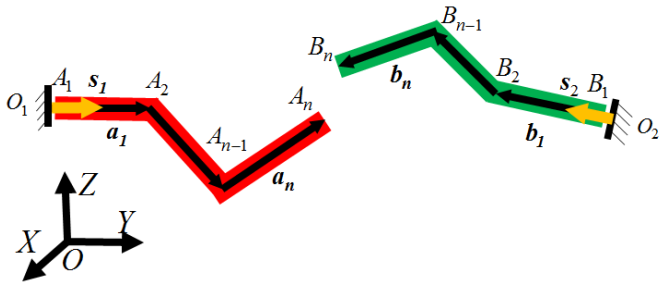


**Figure 2** Representation method of pipe assembly in vectorization.

### 3.2. Assembly modeling

In the actual assembly process, there is a great difference between the ideal pipe assembly model and the actual situation. As shown in Figure 3, the dotted line represents the theoretical installation position of pipe 2. There is angle error and clearance at the butt joint of the pipe after installation due to the deviation of the fixed structure of the pipe. To solve the influence of structural error on the assembly accuracy of the pipe, it is necessary to model the assembly environment of pipe combined with assembly error.

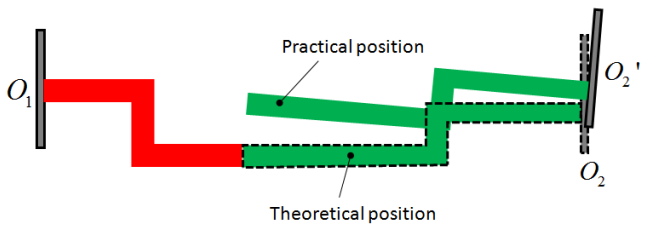


**Figure 3** Sketch of pipe assembly model.

Figure 4 shows the pipe vector model under the structural error environment. When the pipe 1 is fixed, the theoretical installation position of the pipe 2 is shown as the dotted line in the figure, which is denoted by the vector set $\boldsymbol{b} = \{\boldsymbol{b}_1, \mathrm{L}\ , \boldsymbol{b}_n\}$, and the actual pipe position vector set is $\boldsymbol{b}' = \{\boldsymbol{b}_1', \mathrm{L}\ , \boldsymbol{b}_n'\}$. In the actual assembly process, first connect the structural point $O_2$ and the start point $B_1'$ of the pipe 2 to ensure that the vector $\boldsymbol{b}_1'$ of the pipe 2 is parallel to the structural axis $\boldsymbol{s}_2$ to form the actual installation state vector $\boldsymbol{b}'$ of the pipe 2. The actual positions of the structural point $O_2$ and the structural axis vector $\boldsymbol{s}_2$ could be directly obtained by measurement. Then, the actual installation position of the pipe 2 is calculated by using the rotation vector method and the theoretical position of pipe 2.

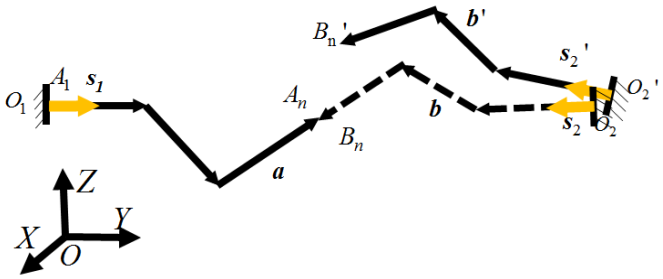


**Figure 4** Vectorized model of pipe assembly in structural error.

The Rodrigues rotation formula is adopted, which uses two elements of space axis vector and rotation angle to transform any vector in space. To ensure that the start vector $\boldsymbol{b}_1'$ of pipe 2 is coaxial with the structural axis $\boldsymbol{s}_2$, calculating the rotation axis and rotation angle of $\boldsymbol{b}_1'$:

(1) Calculate rotation axis $\boldsymbol{e}_{P_1}$

$$\boldsymbol{e}_{P_1} = \frac{\boldsymbol{s}_2' \times \boldsymbol{b}_1}{\mathrm{norm}(\boldsymbol{s}_2 \times \boldsymbol{b}_1)} \tag{5}$$

(2) Calculate rotation angle $\alpha$

$$\alpha = \arccos\left(\frac{\boldsymbol{s}_2 \cdot \boldsymbol{b}_1}{|\boldsymbol{s}_2||\boldsymbol{b}_1|}\right) \tag{6}$$

Then, establish the pipe 2 rotation model and calculate the transformed vector of the pipe 2.

$$\boldsymbol{b}' = \boldsymbol{b}\cos\alpha + (\boldsymbol{e}_{P_1} \times \boldsymbol{b})\sin\alpha + \boldsymbol{e}_{P_1}(\boldsymbol{e}_{P_1} \cdot \boldsymbol{b})(1 - \cos\alpha) \tag{7}$$

where $\mathrm{norm}(\cdot)$ represents the calculation of the vector norm, $\boldsymbol{e}_{P_1}$ is the unit vector of the rotation axis, $\alpha$ is the rotation angle.

## 4. Error Compensation Method

### 4.1 assembly scenario analysis

According to the actual assembly scene, the assembly is divided into single constraint assembly and associated constraint assembly, as shown in Figure 5. Figure 5 (a) shows a single constraint assembly where each segment of the pipe receives only constraints from a single structure. Figure 5 (b) shows the assembly of associative constraints, in which common constraints constrain at least one segment of the pipe from different structures. For example, the $B_3-B_4$ segment of the pipe is constrained by the distance of $d_1$ and $d_2$ at simultaneously.

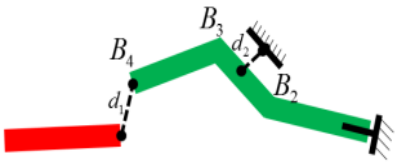


(a) Single constraint

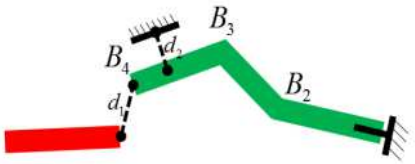


(b) Associated constraint

**Figure 5** Scene analysis on assembly's constraints.

### 4.2 Compensation process

Figure 6 shows the pipe assembly error compensation process, including:

(1) Calculate and judge the key assembly features that need to be compensated;

(2) Compensate the single constraint feature and the associated constraint feature separately and determine the compensated pipe parameters.

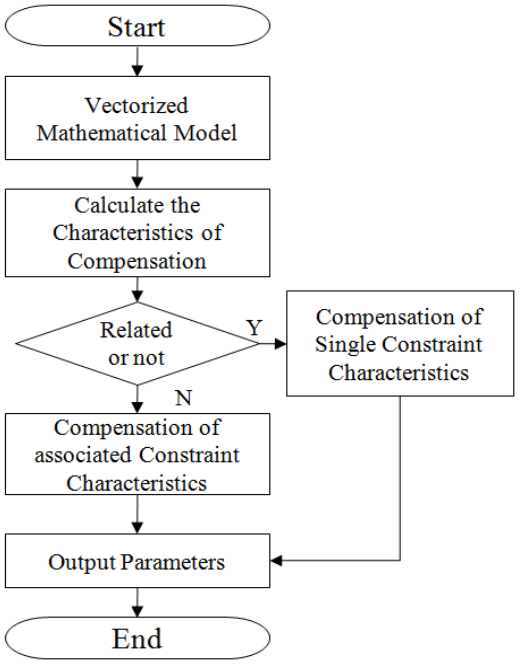


**Figure 6** Flow chart of Error Compensation Technique (ECT).

*4.2.1 Calculate compensation characteristics*

Before compensation, the key assembly features to be compensated are identified. The boundary conditions of the above five features are expressed as $E_1$, $E_2$, $E_3$, $E_4$, $E_5$, as shown in Table 1.

**Table 1** Boundary condition allowance comparison.

| | Name of characteristics | Theoretical value | Allowance |
|---|---|---|---|
| $E_1$ | Angle constraint $\theta_1$ | 0 | $\leqslant[\theta_1]$ |
| $E_2$ | Distance constraint $d_1$ | 0 | $\leqslant[d_1]$ |
| $E_3$ | Angle constraint $\theta_2$ | 0 | $\leqslant[\theta_2]$ |
| $E_4$ | Distance constraint $d_2$ | 0 | $\leqslant[d_2]$ |
| $E_5$ | Distance constraint $d_3$ | $h*$ | $\leqslant[d_3]$ |

According to the method described in Section 2, the pipe points and vector set could be expressed as $\boldsymbol{b}'=\{B_1', \boldsymbol{b_I}', ..., \boldsymbol{b_n}'\}$, where $B_1'$ represents the coordinates of the pipe vector start point, and $\boldsymbol{b_i}'$, $i\in[1,n]$ represents the vector of each linear segment. The calculation method is as follows:

(1) Calculate boundary condition $E_1$, tolerance range $[\theta_1]$:

$$E_1=\arccos\left(\frac{\boldsymbol{b_n}'\cdot\boldsymbol{b_n}}{|\boldsymbol{b_n}'|\cdot|\boldsymbol{b_n}|}\right) \tag{8}$$

(2) Calculate boundary condition $E_2$, tolerance range $[d_1]$:

$$E_2 = \left| \sum_{i=1}^{n} (B_1' + \boldsymbol{b}_i') - \sum_{i=1}^{n} (B_1 + \boldsymbol{b}_i) \right| \tag{9}$$

(3) Calculate boundary condition $E_3$, tolerance range $[\theta_2]$:

$$E_3 = \arccos\left( \frac{\boldsymbol{b}_k' \cdot \boldsymbol{b}_k}{|\boldsymbol{b}_k'| \cdot |\boldsymbol{b}_k|} \right) \tag{10}$$

where $\boldsymbol{b}_k'$ and $\boldsymbol{b}_k$ represent the actual pipe and the theoretical pipe $k-$th vector connected with the clamp respectively.

(4) Calculate boundary condition $E_4$, tolerance range $[d_2]$

$$E_4 = \left( G - \sum_{i=1}^{k} (A_1' + \boldsymbol{b}_i') \right) \cdot \boldsymbol{b}_k' / |\boldsymbol{b}_k'| \tag{11}$$

(5) Calculate boundary condition $E_5$, tolerance range $d_3 - [d_3]$

$$E_5 = \min\left\{ \left[ h_1 + l\overrightarrow{h_1 h_2} - \sum_{i=1}^{j} (B_1' + \boldsymbol{b}_i') \right] \cdot \frac{\boldsymbol{b}_j'}{|\boldsymbol{b}_j'|} \right\} - d_3 \tag{12}$$

where $k$ is the $k-$th vector of the pipe, which may lead to the clearance value dissatisfying the requirements, $\boldsymbol{h_1}$ and $\boldsymbol{h_2}$ are the two points of the surrounding structure, $l$ is the length factor, and $0 \le l \le 1$.

*4.2.2 Single constraint compensation*

The vector model of pipe assembly in single constraint scene is compensated, and the feature error is compensated according to the importance of factors, which influence assembly. Firstly, the pipe is divided into separate linear segments for compensation, and then the linear segments are combined to form a complete compensation model based on assembly features.

(1) Eliminate the error of connecting pipe 1 and pipe 2

The assembly features involved in this step include angle constraint $\theta_1$ and distance constraint $d_1$. Figure 7 (a) shows the error compensation of feature $\theta_1$ and $d_1$. The specific compensation process is to adjust the end vector $\boldsymbol{b_n'}$ of the pipe 2 by translation and rotation transformation so that it is coaxial with the end vector $\boldsymbol{a_n}$ of the pipe 1 and connected head to end, expressed as:

$$\begin{cases} \boldsymbol{b_n}^{(1)} = k\boldsymbol{a_n} \\ \left|\boldsymbol{b_n}^{(1)}\right| = \left|\boldsymbol{b_n'}\right| \\ B_n^{(1)} = A_n \end{cases} \tag{13}$$

where $B_n^{(1)}$ represents the end point of pipe 2 after compensation, $A_n$ represents the end point of pipe 1, and K is a constant.

(2) Eliminate the error between the fixed clamp and the pipe

The assembly features involved in this step include angle constraint $\theta_2$ and distance constraint $d_2$. Figure 7 (b) shows the error compensation of feature $\theta_2$ and $d_2$. Adjust the vector $\boldsymbol{b_j'}$ of the straight line segment matched with the pipe 2 to make it coaxial with the clamp axis vector $\overrightarrow{g_1 g_2}$, and pass through the clamp center point $G$, and the distance between the vector endpoint and the point $G$ is kept equal, expressed as:

$$\begin{cases} \boldsymbol{b_j}^{(1)} = r\overrightarrow{g_1 g_2} \\ \left|\boldsymbol{b_j}^{(1)}\right| = \left|\boldsymbol{b_j'}\right| \\ \left|\boldsymbol{B_j}^{(1)} - G\right| = \left|\boldsymbol{B_j'} - G\right| \end{cases} \tag{14}$$

where $\boldsymbol{b_j}'$, $\boldsymbol{b_j}^{(1)}$ are the $j$ vector of pipe 2 before and after compensation, $B_j'$ and $B_j^{(1)}$ are the endpoint of the $j$ vector of pipe 2 before and after compensation, $r$ is a constant, indicating that the vector $\boldsymbol{b_j}^{(1)}$ is parallel to $\overrightarrow{g_1 g_2}$.

(3) Combination after compensation

After the compensation of (1) and (2) above, the pipe vector of each straight line segment has met the requirements of assembly features. On this basis, to ensure that the vector direction remains unchanged, adjust the vector size to fit and generate the pipe 2 model. Figure 7(c) shows the compensation result of pipe 2.

$$\begin{cases} B_n^{(1)} - \boldsymbol{b_n}^{(2)} = B_i^{(1)} + k_1 \boldsymbol{b_i}^{(1)} \\ B_i^{(1)} - (1 + k_2 \boldsymbol{b_i}^{(1)}) = B_1 + \boldsymbol{b_1}^{(2)} \\ \boldsymbol{b_i}^{(2)} = (k_1 + k_2 + 1)\boldsymbol{b_i}^{(1)} \end{cases} \tag{15}$$

where $k_1$, $k_2$ are constant parameters. Eq. (15) gives the complete vector expression of the compensated pipe 2, express as $\boldsymbol{b}^{(2)} = \left\{ \boldsymbol{b_1}^{(2)}, ..., \boldsymbol{b_n}^{(2)} \right\}$.

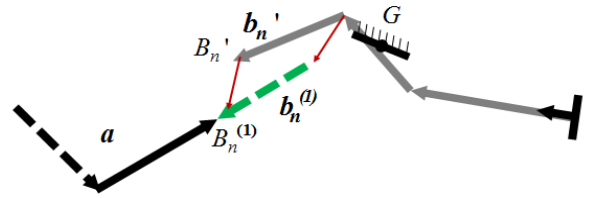


(a) Compensate the characteristics of $\theta_1$ and $d_1$

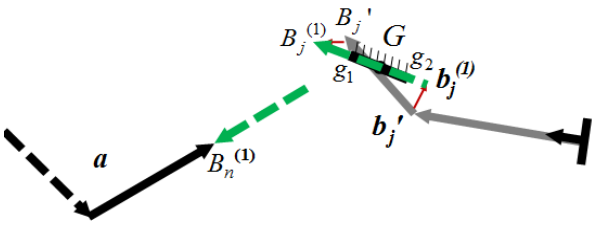


(b) Compensate the characteristics of $\theta_2$ and $d_2$

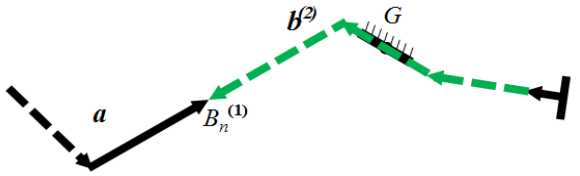


(c) Combination after compensated

**Figure 7** ECT sketch of main characteristics of pipe assembly.

*4.2.3 Associative constraint compensation*

When two key features need to be compensated on the same vector, if one feature is fully compensated, other features may exceed the allowable value range and cannot be compensated. Figure 8 shows the conflict of the angle and distance error between the clamp and the pipe 2 at the butt joint. Where $\beta_1 \sim \beta_4$ represents the angle between the clamp axis and the j-th vector of pipe 2 after compensation, the angle between the end vector of pipe 1 and the j-th vector of pipe 2 after compensation, the angle between the clamp axis and the end vector of pipe 1, and the angle between the end vector of pipe 1 and the j-th vector of pipe 2 before compensation, and $d_1'$, $d_2'$ represents the distance between the end point of pipe 2 and the end of pipe 1 after compensation, and the distance between the straight line segment of pipe 2 and the center point of the clamp after compensation. The specific calculation process is as follows:

(1) Calculating $\beta_2 \sim \beta_4$:

$$\begin{cases} \beta_3 = \arccos\left(\dfrac{\overrightarrow{g_1g_2}\cdot \boldsymbol{a_n}}{\left|\overrightarrow{g_1g_2}\right|\left|\boldsymbol{a_n}\right|}\right) \\ \beta_4 = \arccos\left(\dfrac{\boldsymbol{a_n}\cdot \boldsymbol{b_j}}{\left|\boldsymbol{a_n}\right|\left|\boldsymbol{b_j}\right|}\right) \\ \beta_2 = \beta_3 - \beta_1 \end{cases} \tag{16}$$

(2) Calculating $d_1'$, $d_2'$:

Calculate the vertical vector of $\boldsymbol{b_j}'$ and $\boldsymbol{a_n}$ according to $\boldsymbol{b_j}$ and $\boldsymbol{a_n}$, Using Rodriguez' formula, the function of $\boldsymbol{b_j}'$ about $\beta_1$ is calculated according to Eq. (7):

$$\boldsymbol{b}(\beta_1)' = \boldsymbol{b}\cos\beta_1 + \left(\boldsymbol{e}_{\boldsymbol{P}_j} \times \boldsymbol{b}\right)\sin\beta_1 + \boldsymbol{e}_{\boldsymbol{P}_j}\left(\boldsymbol{e}_{\boldsymbol{P}_j}\cdot \boldsymbol{b}\right)(1-\cos\beta_1) \tag{17}$$

Then, calculating $d_1'$ and $d_2'$

$$\begin{cases} d_1' = \left|B' - A\right| \\ d_2' = \overrightarrow{G-B'}\cdot \boldsymbol{b}_j'/\left|\boldsymbol{b}_j'\right| \end{cases} \tag{18}$$

Simultaneous solving:

$$\begin{cases} d_1' \le [d_1] \\ d_2' \le [d_2] \\ \beta_1 \le [\theta_1] \\ \beta_2 \le [\theta_2] \end{cases} \tag{19}$$

where $[d_1]$, $[d_2]$, $[\theta_1]$, $[\theta_2]$ represent the allowable values of angle constraints $\theta_1$, $\theta_2$ and distance constraints $d_1$, $d_2$, respectively.

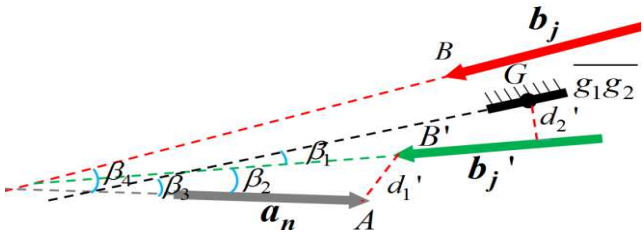


**Figure 8** ECT sketch of differentiated main characteristics.

Bring the solution result of Eq. (19) into Eq. (17) to obtain the theoretical vector model of pipe 2 after compensation.

## 5. Experiment and analysis

To verify the proposed pipe error compensation method, Figure 9 shows the theoretical installation structure of two flared pipes. The pipe 1 and the pipe 2 are connected at the middle part by a pipe joint, and the end of the pipes and the middle parts are constrained by the aircraft structure. Figure 10 shows the partial connection structure of the pipe, where the flared part of the pipe and the tapered surface of the pipe joint and the tapered surface of the flat nozzle form a seal through the extrusion of the jacket nut, and the jacket nut and the pipe joint are threaded to generate axial pretension.

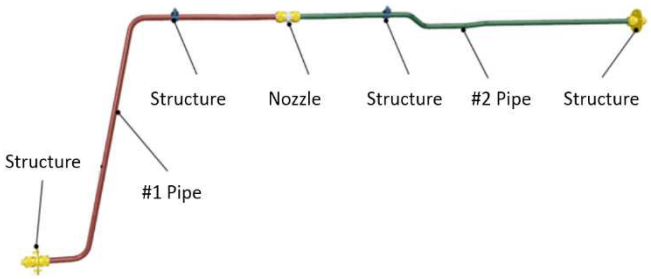


**Figure 9** Structure of experimental pipe assembly.

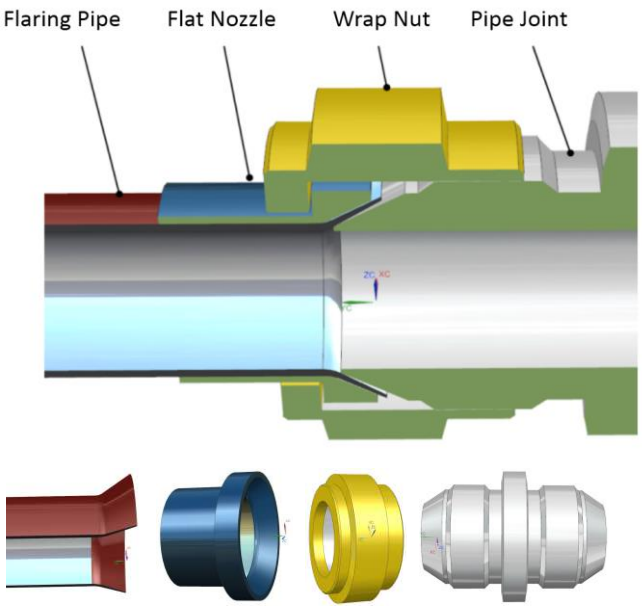


**Figure 10** Connected structure of partial pipe assembly.

Table 2 shows the theoretical model parameters of pipe 1 and pipe 2 based on the aircraft coordinate system. Table 3 shows the configuration parameters of the two pipes installation structure, including the coordinate values of the end points of structure 1 and structure 2, the end vectors of structure 1 and structure 2, and other related constraints.

**Table 2** Parametric model of #1 pipe and #2 pipe (Theoretical).

| | Point | X | Y | Z |
|---|---|---|---|---|
| #1 Pipe | $A_1$ | -50 | 4109 | 100 |
| | $A_2$ | -50 | 4182.38 | 100 |
| | $A_3$ | 366.95 | 4279.77 | 51.02 |
| | $A_4$ | 366.95 | 4557.01 | 44.88 |
| #2 Pipe | $B_1$ | 350 | 5312.17 | 50 |
| | $B_2$ | 350 | 4986.45 | 50 |
| | $B_3$ | 350 | 4951.62 | 70 |
| | $B_4$ | 350 | 4861.49 | 70 |
| | $B_5$ | 366.95 | 4821.14 | 39.03 |
| | $B_6$ | 366.95 | 4596.69 | 44 |

**Table 3** Parameters of experimental pipe in structure part.

| | X | Y | Z |
|---|---|---|---|
| Structure 1 vertex $O_1$ | -50.00 | 4109.00 | 100.00 |
| Vector $\boldsymbol{s_1}$ | 0 | 1 | 0 |
| Structure 2 vertex $O_2$ | 348.54 | 5311.55 | 50.10 |
| Vector $\boldsymbol{s_2}$ | -0.003 | 1 | 0.001 |
| Starting point $h_1$ | 582 | 4457 | 0 |
| Vector $\overrightarrow{h_1h_2}$ | -1164 | 0 | 0 |
| Vector $\overrightarrow{g_1g_{21}}$ | 0 | -13 | 0 |
| Midpoint $G$ | 366.23 | 4363.31 | 49.2 |
| Vector $\overrightarrow{g_1g_{22}}$ | 0 | -13 | 0.29 |
| Midpoint $G_2$ | 365.5 | 4655.32 | 42.79 |

### 5.1 Calculation of compensation

According to the proposed compensation method, the pipe is calculated. According to the theoretical model axis vectors of pipe 1 and pipe 2 extracted from Table 2 and the installation structure axis vector measured in Table 3, the pipe 2 pose adjustment based on assembly features was carried out. Firstly, the angle between the $\boldsymbol{b}_1$ vector of pipe 2 and the axis vector of the installation structure is calculated by using Eq. (5) to Eq. (6). Then the vector set after the rotation of pipe 2 is calculated by Eq. (7). Finally, the start point $B_1'$ of pipe 2 is translated to coincide with the end point of structure 2.

According to the calculation, the distance between the end points of pipe 2 before and after adjustment is as

follows:

$$\Delta d_{B6} = \left| B_6 - B_6{}' \right| = 1.5893mm \tag{20}$$

The angle between the vector and the vector:

$$\Delta\theta_{b5} = \arccos\frac{\boldsymbol{b}_5 \cdot \boldsymbol{b}_5{}'}{|\boldsymbol{b}_5||\boldsymbol{b}_5{}'|} < 1\times10^{-4} \qquad 20)$$

Then, according to Eq. (8) to Eq. (14) and combined with the key assembly characteristic parameters given in Table 3, the pipe 1 is compensated. Table 4 shows the parameters of pipe 1 after compensation, Figure 11 shows the theoretical model of pipe assembly and Figure 12 shows the state of pipe 1 after compensation.

**Table 4** Parametric model of adjusted #2 pipe and compensated 1# pipe.

| Point | X | Y | Z |
|---|---|---|---|

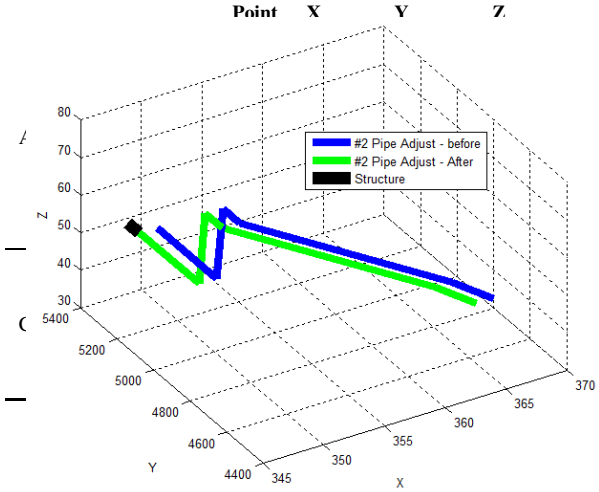


**Figure 11** Theoretical model of pipe assembly.

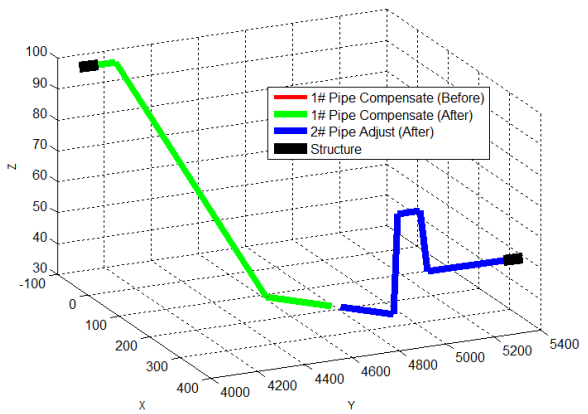


**Figure 12** Before-and-after compensation sketch of pipe.

By using the rotation vector method to adjust the position and pose of the pipe 2, and to compensate the error of the pipe 1 based on the assembly features, it can be found that:

(1) The proposed method can effectively realize the position and posture adjustment of pipe 2. Besides, it could be found that the distance deviation between the two endpoints of pipe 2 before and after adjustment is 1.5893mm, and the angle deviation is less than $1\times10^{-4}$ degree;

(2) Compared with Table 2 and Table 3, it could be found that the state of pipe 1 has changed before and after compensation.

### 5.2 Air tightness experiment

Two groups of pipes before and after compensation were selected for installation and air tightness test. Figure 13 shows the pre-assembly effect of the pipe before and after compensation, and Figure 13(a) shows the pre-assembly drawing before compensation, in which there is large stress between the pipe joint and the two pipes, resulting in obvious deviation of the axis of the pipe joint and the end of the pipe. Figure 13 (b) shows the installation drawing of the compensated pipe, in which the fitting degree between the pipe joint and the two pipes is better.

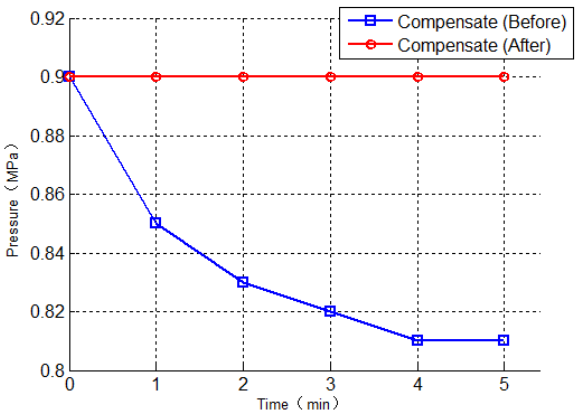


**Figure 14** Before-and-after airtightness photo after compensated #1 pipe.

According to the Chinese aviation industry standard

HB4-1-2002 "General Specification for Flared Pipe Connections", the first step is using a wrench with constant torque of 60 N/m to install the pipe. According to the assembly air tightness requirements, the second step is inflating the assembled pipe to make the internal pressure of the pipeline reach 0.9Mpa, and maintaining the pressure for 5 min to observe the change of the pipeline pressure. Figure 14 shows the change of the air pressure value of the two groups of pipes during the pressure maintaining period. It could be found that the two groups of pipes have pressure relief before the error compensation, and the internal pressure of the compensated pipe is constant. The air tightness test shows that the proposed error compensation method could avoid the assembly problems caused by the installation environment and improve the air tightness of the pipe assembly.

## 6. Conclusions

In this paper, the vector model of the pipe assembly process is established, and methods of compensating the assembly error under the single constraint and the associated constraint are proposed respectively. The compensation method is verified by calculating the pipe assembly error compensation and the air tightness test of the pipe. The results show that:

(1) The proposed method can effectively realize the space pose adjustment of the pipe. Through calculation, the distance compensation between the two endpoints of the pipe is 1.5893*mm*, and the angle compensation is less than $10^{-4}$ degree.

(2) The air tightness of the compensated duct is better than that of the uncompensated one.

In this paper, the pipeline assembly error compensation method validation under the single constraint environment is tested. The follow-up work will further research and verifying of the pipeline assembly error compensation method under the associated constraints and other complex constraints.

## 7 Declaration

**Acknowledgements**

This work was supported by the National Key R&D Program of China under Grant 2017YFB1301700.

**Authors' contributions**

The author' contributions are as follows: Wen-Xiang Gao was in charge of the whole trial; Yu-long Lan wrote the manuscript; Bang-Yi Li was in charge of the experimental design; Song-Lin Chen assisted with sampling and laboratory analyses; Mu-Tian Tang is responsible for translating and revising grammar.

**Competing interests**

The authors declare that they have no known competing financial interests or personal relationships that could have appeared to influence the work reported in this paper.

**Consent for publication**

Not applicable

**Ethics approval and consent to participate**

Not applicable

**References**

[1] W Fan, L Y Zhang, Y H Wang. Automatic reconfigurable and flexible fixture system for pipeline components in assembly process. Computer Integrated Manufacturing Systems 2018; 24(11):38-52. (in Chinese)

[2] H Gong，H Jiang，G Bian. Calculation and analysis of aircraft fuel line flexible coupling leakage. Science Technology and Engineering 2019;19( 25) : 358-363. (in Chinese)

[3] S Shu, X Fan, F Liu, et al. Fracture Failure Analysis and Improvement Verification of Elbow Tube in a Certain Type of Aircraft［J］.Machine Tool & Hydraulics 2019; 47( 2) :176 －180. (in Chinese)

[4] H Shi. Study on safety Design and Leakage Detection Technology of the Aircraft Pneumatic Duct System[dissertation]. Nanjing University of Aeronautics and Astronautics;2013. (in Chinese)

[5] W G Yu, G Chen, B B Liu, et al. Design of a particle damping absorber and experimental study on vibration damping of the pipe[ J]. Chinese Journal of Aeronautics 2018; 39(12):422264. doi:10.7527/S1000 - 6893.2018.22264. (in Chinese)

[6] Z X Wang, M X Qiu, J J Wang. Sealing performance of pipeline connection under the tensile load. Journal of Aeros pace Power 2011;26(08):1866-1870. (in Chinese)

[7] G Chen, Y Luo, Q H Zheng, et al. Fluid-structure coupling dynamic model of complex spatial fluid-conveying pipe system and itsverification. Acta Aeronautica et Astronautica Sinica 2013;34(3):597-609. (in Chinese)

[8] F F Song, H Yang, H Li, M Zhan, Y Wang, G J Li. Significance Analysis of Processing Parameters Effect on Springback in High Strength TA18 Tube NC Bending. RARE METAL MATERIALS AND ENGINEERING 2013;42(01):43-48. (in Chinese)

[9] A V Balaykin, K A Bezsonov, M V Nekhoroshev, A P Shulepov. Developing Parametric Models for the Assembly of Machine Fixtures for Virtual Multiaxial CNC Machining Centers 2018. IOP Conference Series Materials Science and Engineerig 302,012009.

[10] Z Y Zhang. Active compensaation of the deviation in the digital assembly and welding of thin-wall aluminum alloy tube[D]. Harbin Institute of Technology.2015.06. (in Chinese)

[11] D B Zeng, J Xu, Z H Shi, Q Wang. Study on Digital and Flexible Positioning Technology of Airplane Pipes.Aeronautical

Manufacturing Technology 2017; 14(No.533):45-8. (in Chinese)
[12] Z Q Zhang. Assembly Precision and Control for Precision Mechanical System [D]. Bejing Institute of Technology 2017. (in Chinese)
[13] X G Han, M R Tian. Error Analysis of Posture Adjustment for Major Part. Aeronautical Manufacturing Technology 2011;(22):112-115. (in Chinese)
[14] L Cheng. Stduy on Key Techniques of Variation Modeling and Coordination for Large Aircraft Digital Assembly Based on Key Characteristics.,Zhejiang University,2014. (in Chinese)
[15] S Ding, X D Huang, C J Yu, W Wang. Actual inverse kinematics for location error compensation of five-axis machine tool 2017;23(10):2156-2163. (in Chinese)
[16] K Manohar, T Hogan, J Buttrick, et al. Predicting shim gaps in aircraft assembly with machine learning and sparse sensing. Journal of Manufacturing Systems 2018;S0278612518300116.
[17] Z C Qi, K F Zhang, Y Li, et al. Analysis and optimization for locating errors of large wing panel during automatic drilling and rive-ting.Acta Aeronautica et Astronautica Sinica 2015;36(10):3439-3449. (in Chinese)
[18] 18. Zhang H, Zhou L, Gao XJ, et al. Application Research of Laser Tracker in Aircraft Manufacturing .Aeronautical Manufacturing Technology 2014; 465(21):96-98. (in Chinese)
[19] J Yu, Y Zhao, S F Niu, H Wang, W Z Qiu. Direct Linearization Method and Its Application in the Assembly of Pipelines of Rocket Engine. JOURNAL OF SHANGHAI JIAO TONG UNIVERSITY 2016;50(6):957-962. (in Chinese)
[20] Yi-Hao, Kang, Bi-Hua, et al. Reverse engineering of a Hamiltonian for a three-level system via the Rodrigues' rotation formula. Laser Physics Letters, 2017.
[21] Q C Xiong, J X Wang, Q H Zhou. Prediction model of machining errors based on precision and process parameters of machine tools. Acta Aeronautica et Astronautics Sinica 2018;39(8):421713. doi:10.7527/S1000-6893.2018.21713. (in Chinese)

## Biographical notes

**Yu-Long LAN** received the B.S. and M.S. degrees from Sichuan University, Sichuan, China in 2000 and 2008 respectively. He is currently pursuing a PhD degree at *Nanjing University of Aeronautics and Astronautics*. Besides, he is an engineer in *AVIC Chengdu Aircraft Industrial (Group) Co., Ltd., Chengdu China*. His main research interests include the technology of aircraft assembly and Integrated Supply Chain (ISC).
E-mail: lanyl_2020@163.com

**Wen-Xiang GAO** received the B.S. and Ph.D. degree from *Sichuan University, Sichuan, China* in 2014 and 2019 respectively. He is currently an engineer in *AVIC Chengdu Aircraft Industrial (Group) Co., Ltd., Chengdu, China*. His main research interests include robot collision-free path planning, aircraft automatic assembling technology, application of industrial robot.
E-mail: gao_scu@163.com

# Figures

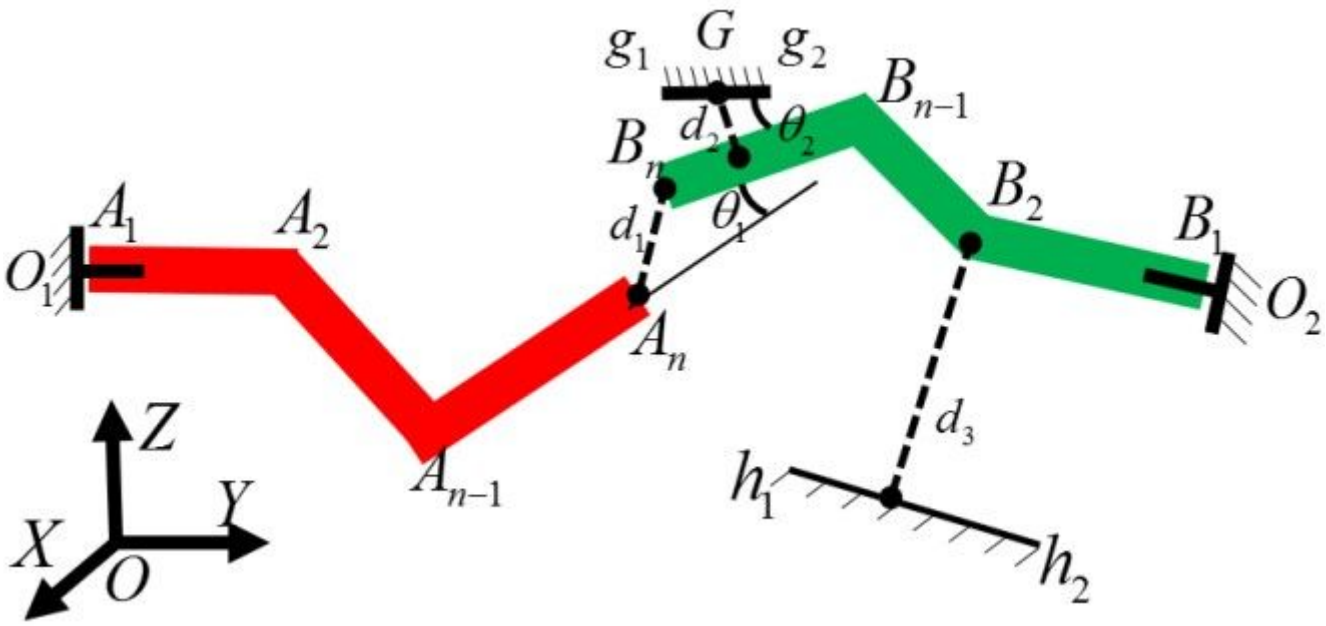


**Figure 1**

2D – Structural assembly sketch of pipeline.

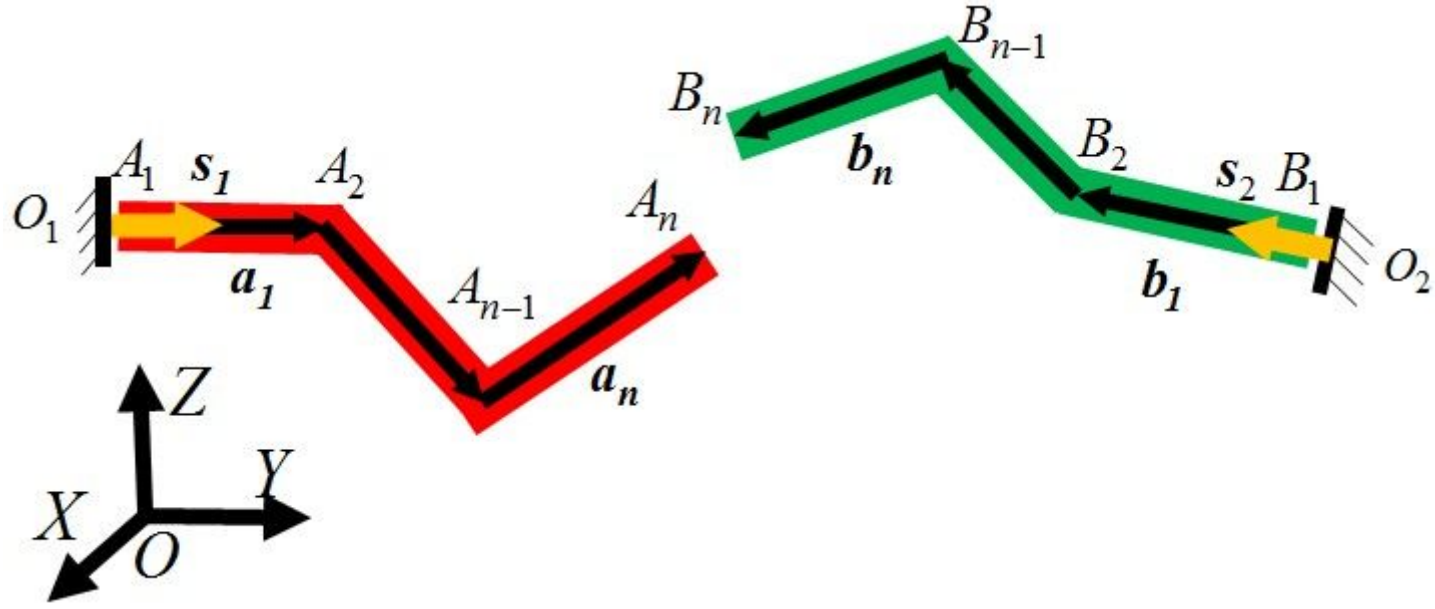


**Figure 2**

Representation method of pipe assembly in vectorization.

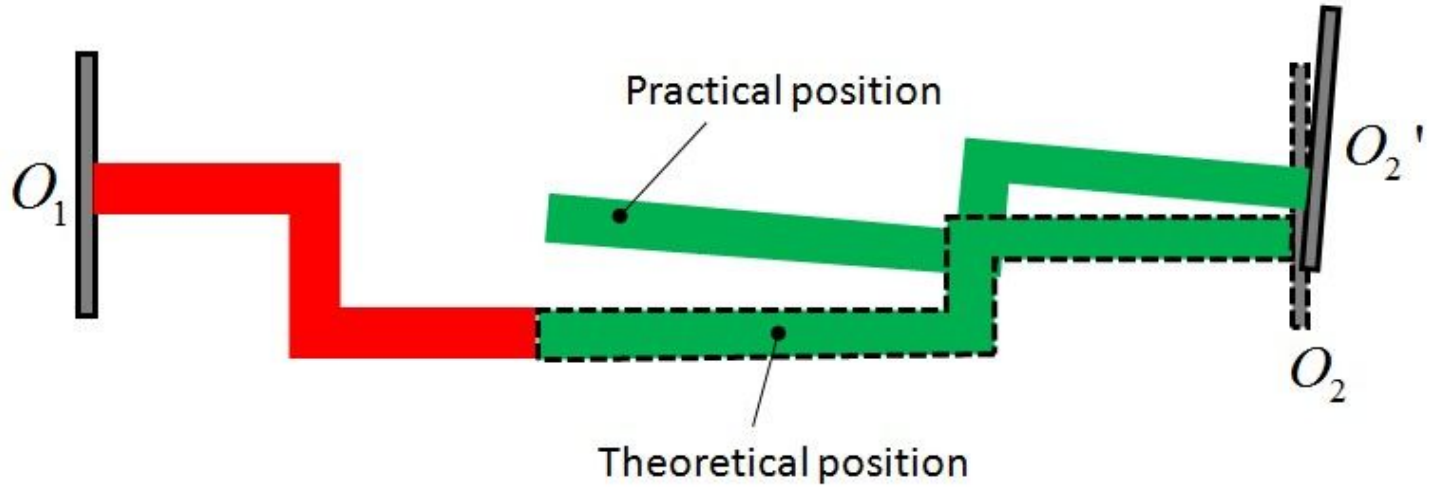


**Figure 3**

Sketch of pipe assembly model.

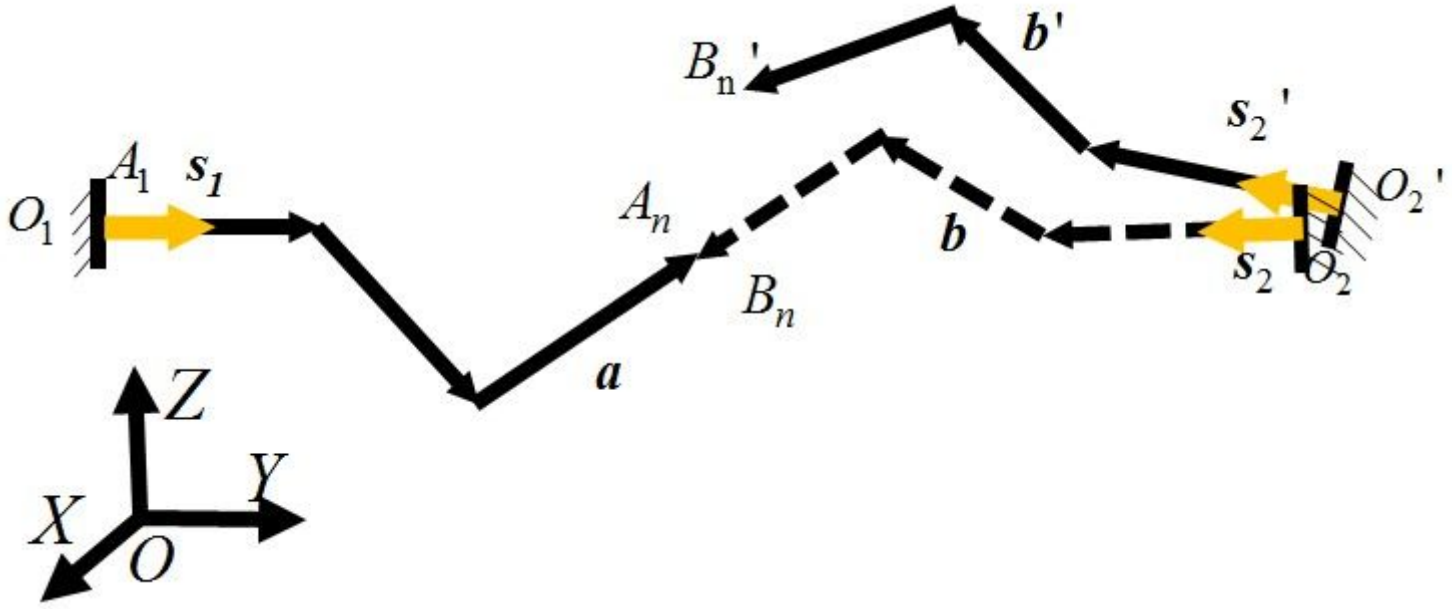


**Figure 4**

Vectorized model of pipe assembly in structural error.

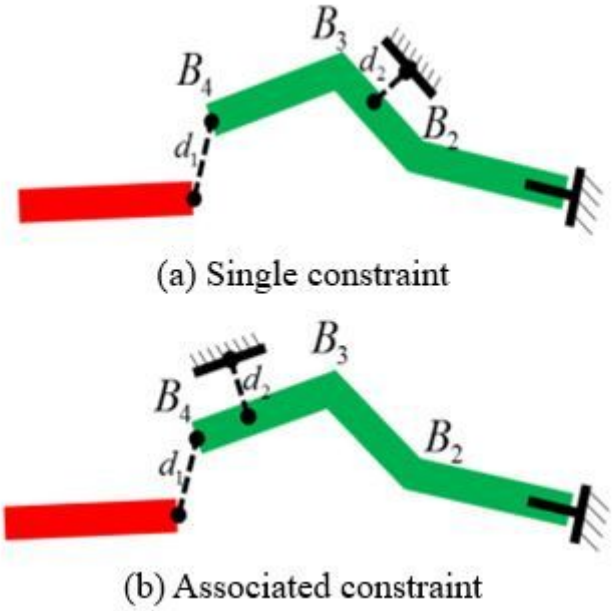


**Figure 5**

Scene analysis on assembly's constraints.

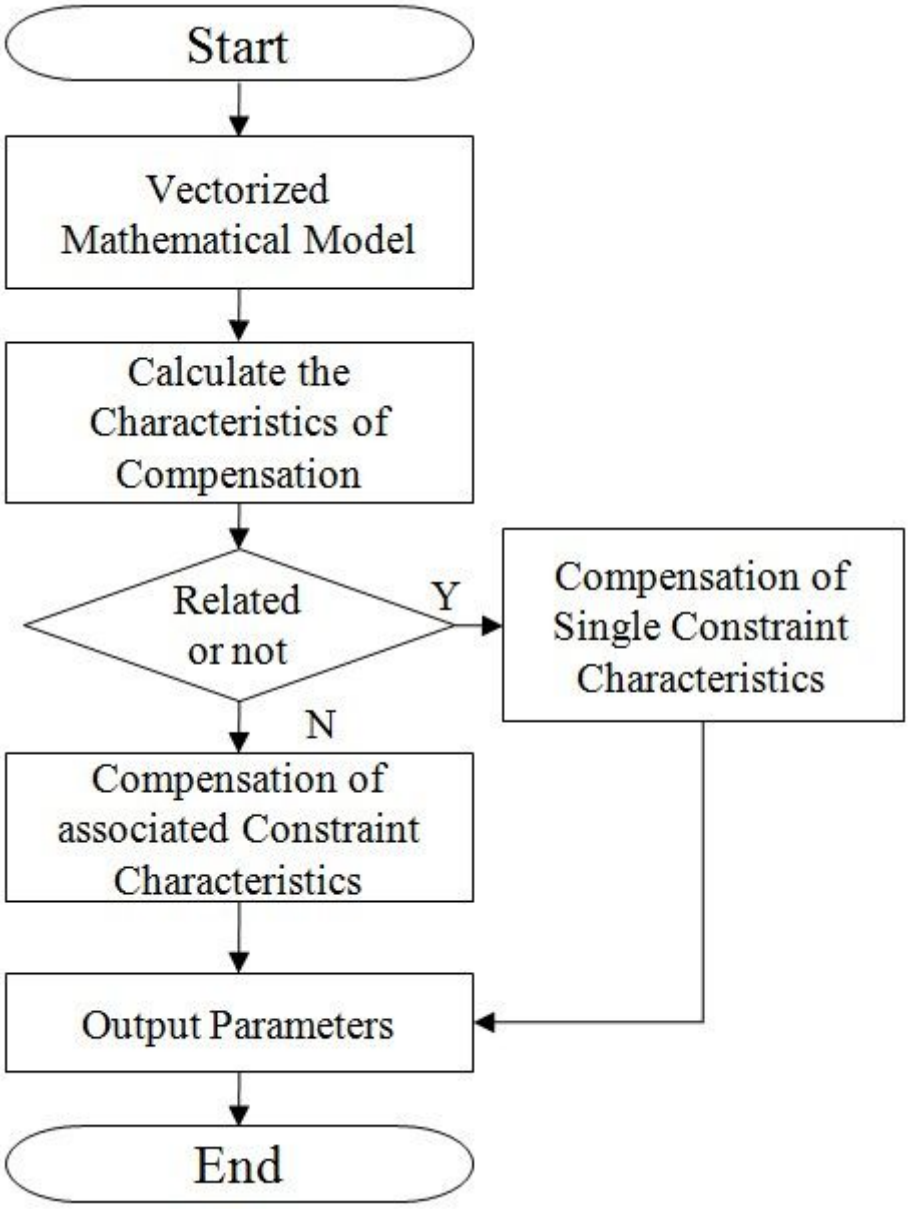


**Figure 6**

Flow chart of Error Compensation Technique (ECT).

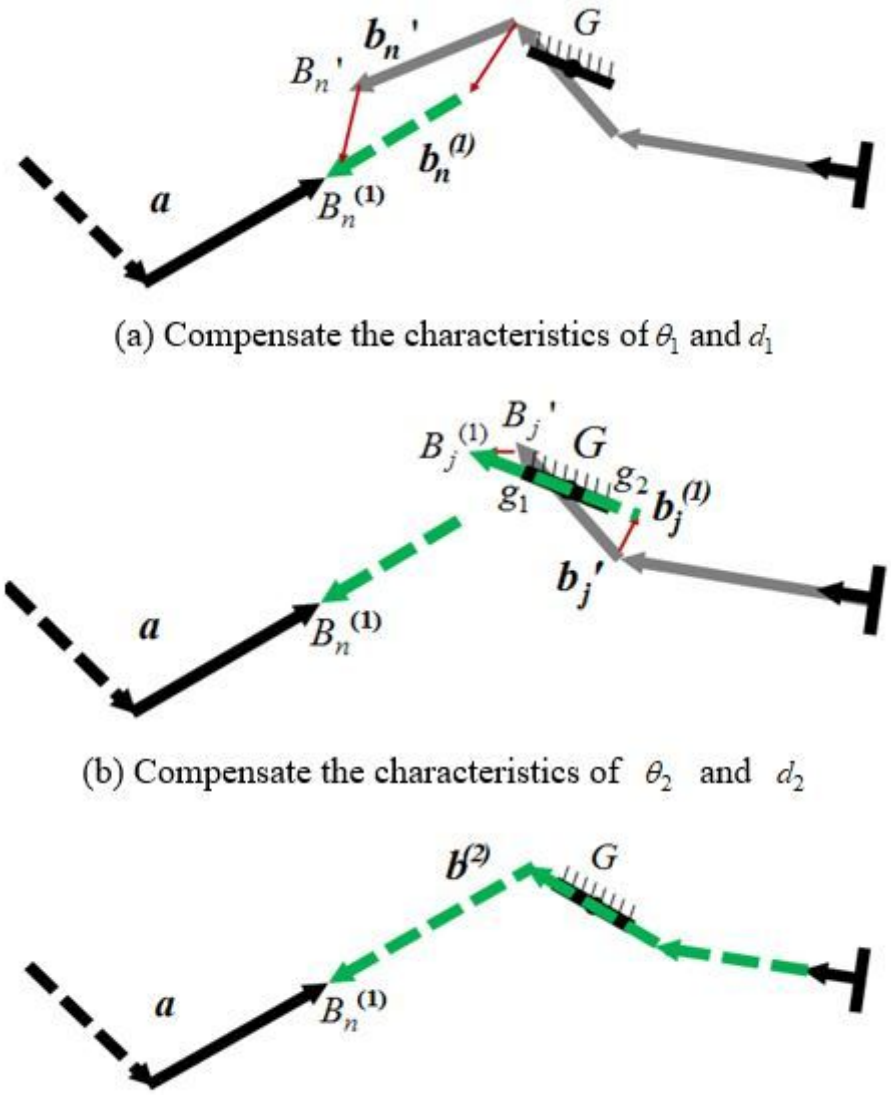


**Figure 7**

ECT sketch of main characteristics of pipe assembly.

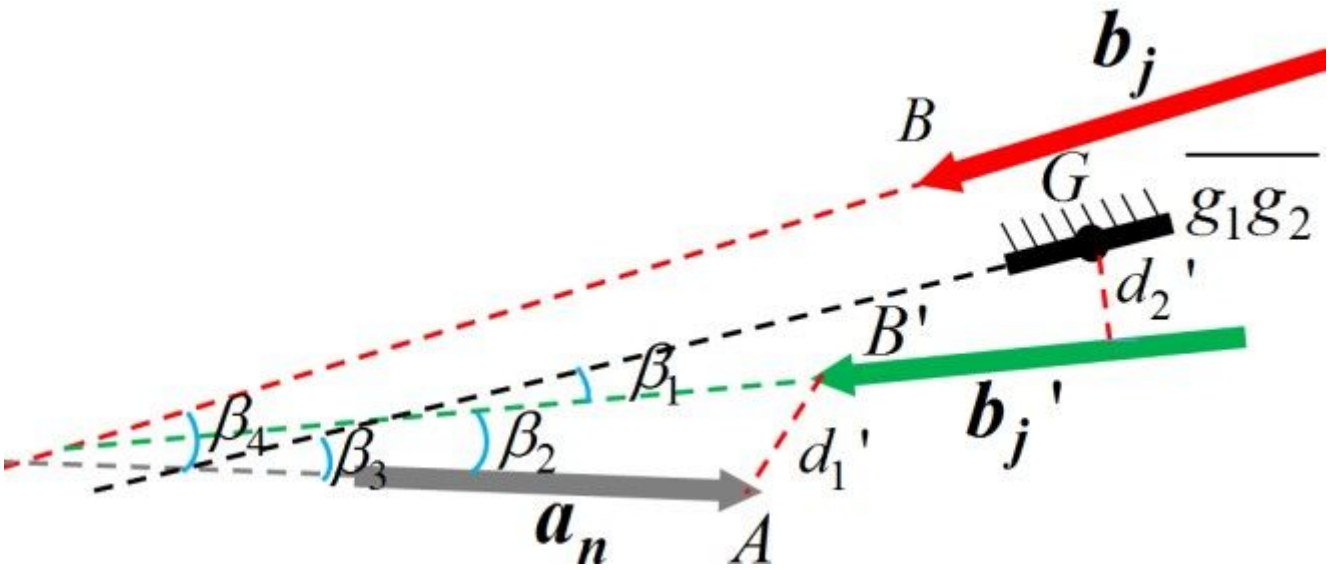


**Figure 8**

ECT sketch of differentiated main characteristics.

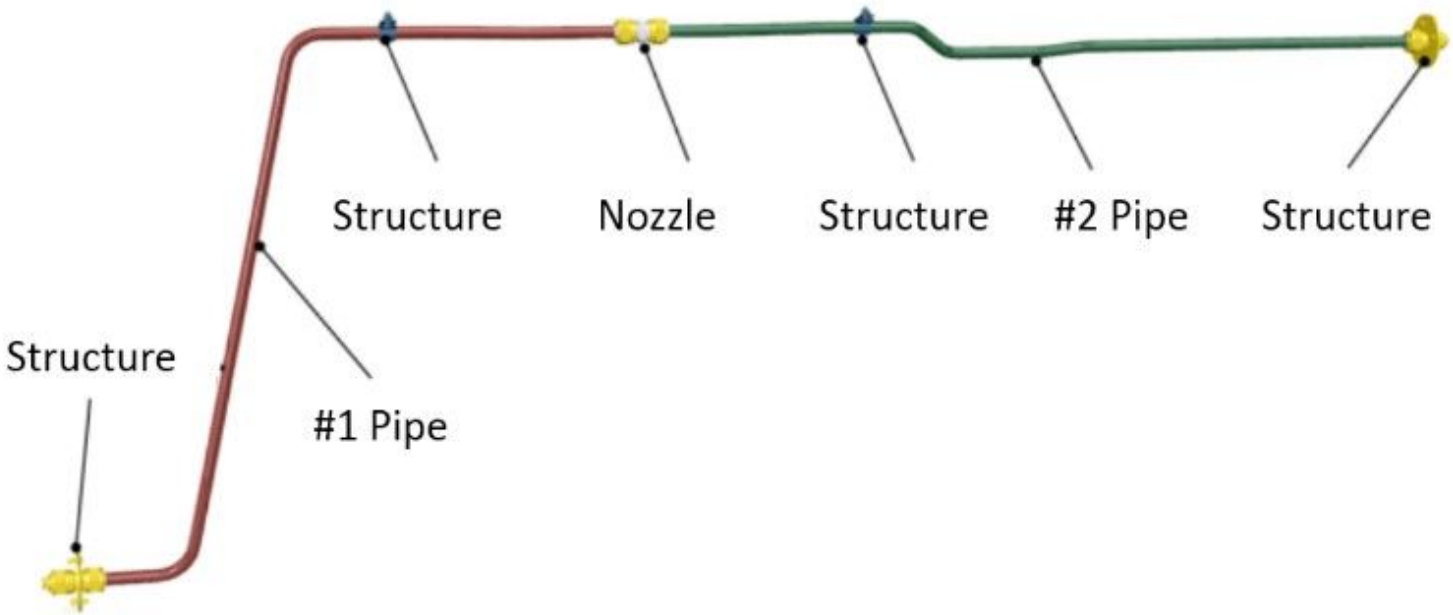


**Figure 9**

Structure of experimental pipe assembly.

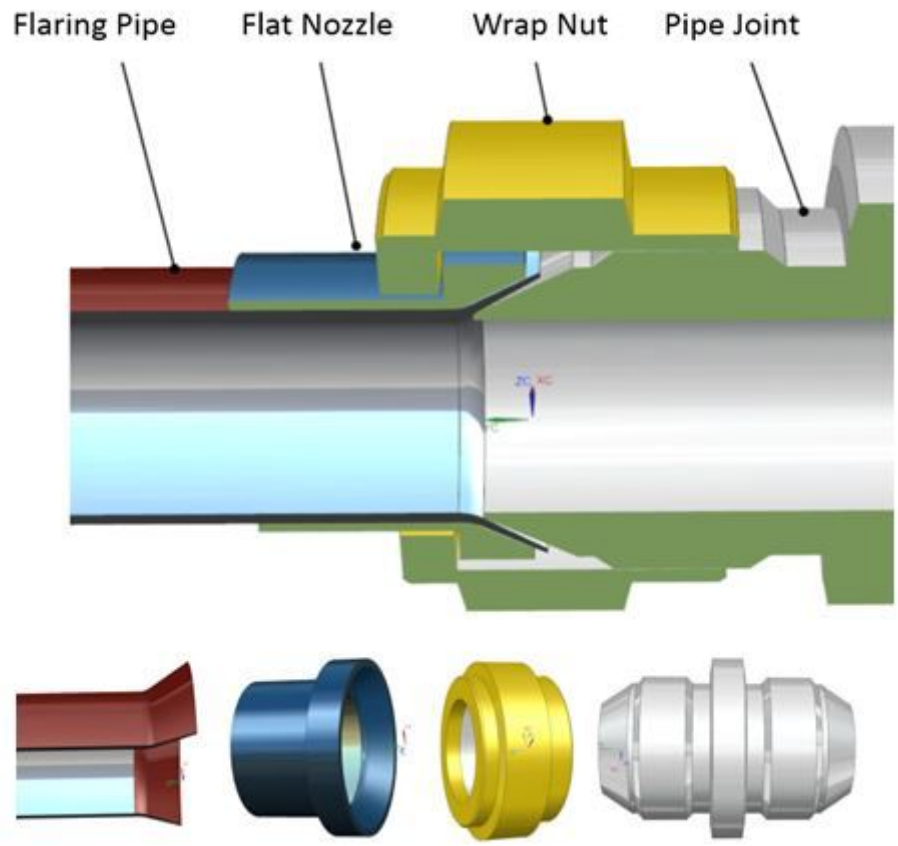


**Figure 10**

Connected structure of partial pipe assembly.

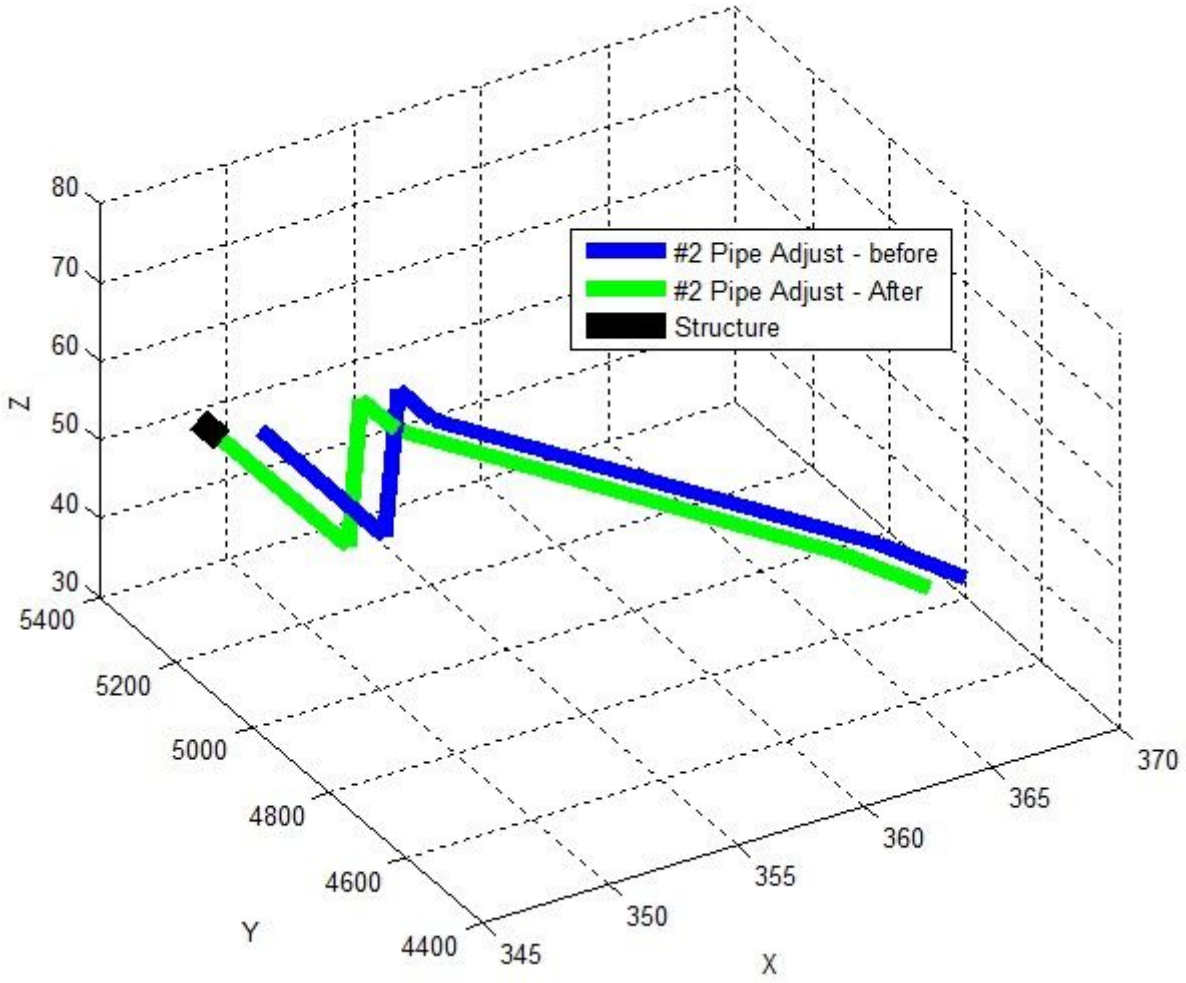


**Figure 11**

Theoretical model of pipe assembly.

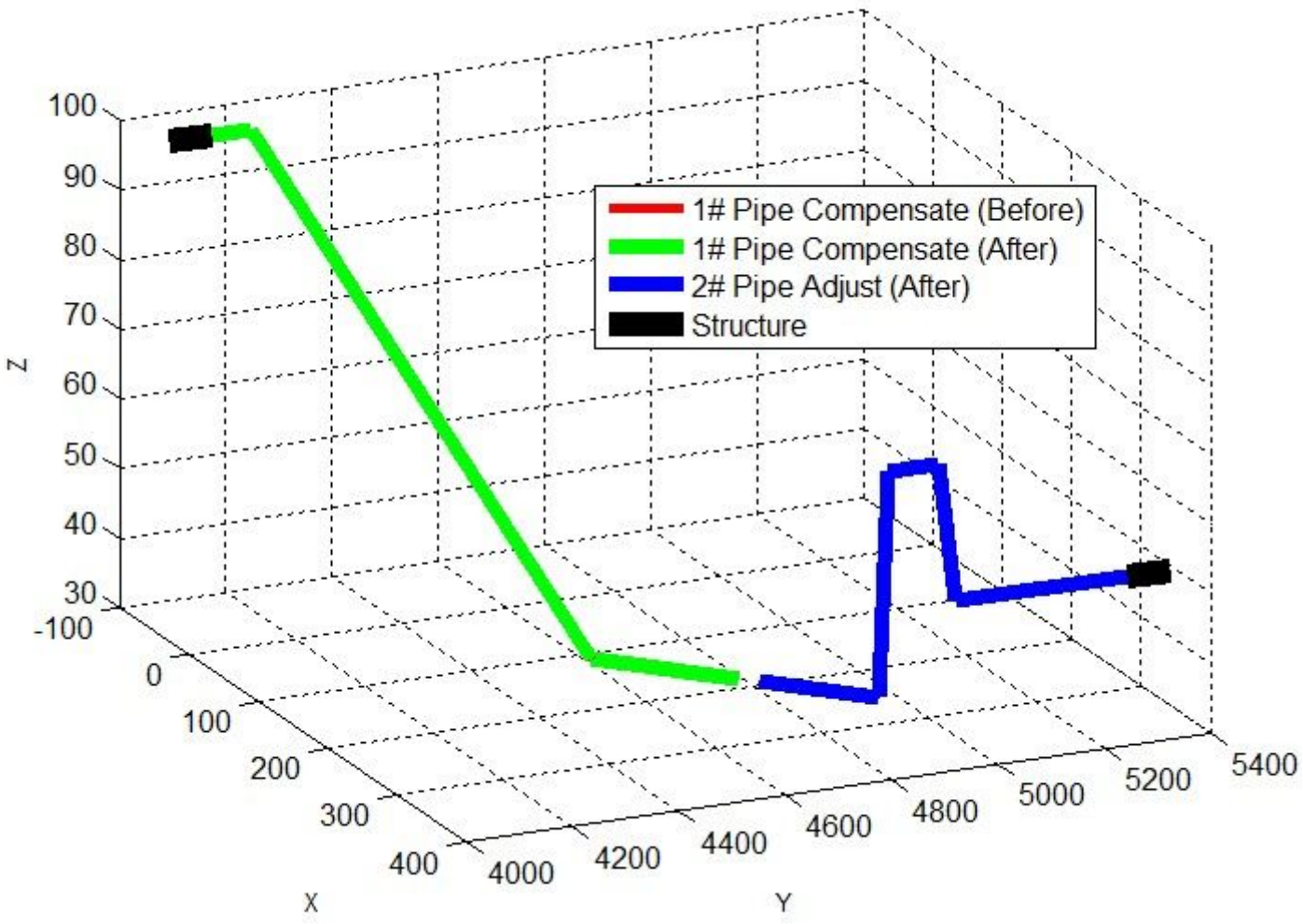


**Figure 12**

Before-and-after compensation sketch of pipe.

Image not available with this version

**Figure 13**

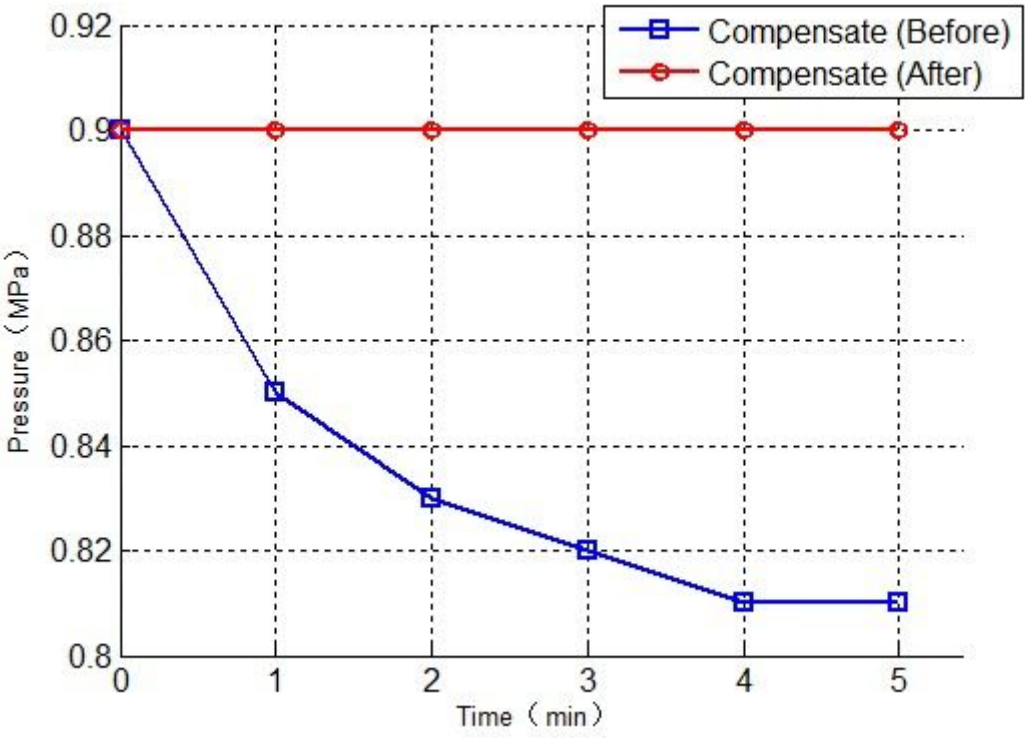


**Figure 14**

Before-and-after airtightness photo after compensated #1 pipe.